

# Brief communication: A simple axial induction modification to WRF's Fitch wind farm parameterisation

Lukas Vollmer<sup>1,\*</sup>, Balthazar Arnoldus Maria Sengers<sup>1,\*</sup>, and Martin Dörenkämper<sup>1</sup>

<sup>1</sup>Fraunhofer IWES, Küpkersweg 70, 26129 Oldenburg, Germany

\*These authors contributed equally to this work.

**Correspondence:** Lukas Vollmer (lukas.vollmer@iwes.fraunhofer.de); Balthazar Sengers (balthazar.sengers@iwes.fraunhofer.de)

**Abstract.** We propose a modification to the Fitch wind farm parameterisation implemented in the Weather Research and Forecasting (WRF) model. This modification, derived from the 1D momentum theory, employs a wind speed-dependent induction factor to correct the local grid wind speed back to free stream, before computing the turbine's power and thrust. While the original implementation underestimates power, the modified version shows a good agreement with the power curve. We strongly recommend the modification to be employed for all studies that model at maximum one turbine per WRF grid cell. For simulations with more turbines per grid cell, additional inner-cell wake losses have to be considered.

## 1 Introduction

As offshore wind energy is developing quickly and in relatively concentrated regions along the coastline, models are needed that correctly represent large-scale wake effects and their interactions with the atmosphere. Several attempts towards the realistic modelling of those effects have been made by employing fast engineering (e.g., Nygaard et al., 2020), high-fidelity (e.g., Wiegant and Verzijlbergh, 2019; Maas and Raasch, 2022) or mesoscale weather models (e.g., Lundquist et al., 2019; Siedersleben et al., 2018). The latter are being used by an increasing number of institutions (Fischereit et al., 2021).

The most commonly used mesoscale model, especially when studying large-scale wake effects, is the Weather Research and Forecasting model (WRF, Skamarock and Klemp, 2008; Skamarock et al., 2021). The wind farm parameterisation proposed by Fitch et al. (2012) has been integrated into WRF's main code for approximately a decade, establishing itself as the most frequently utilized approach (Fischereit et al., 2021). It models wind farms as an elevated sink of momentum and a source of turbulent kinetic energy, assuming that thrust that is not converted to power linearly scales with the turbulence added to the flow.

The Fitch parameterisation does not consider the effect induction has on the local wind speed at the grid cell of the turbine. In this publication we show that, as a consequence, the turbines' power and thrust are underestimated. Abkar and Porté-Agel (2015) mention that the local wind speed may deviate from the free wind speed that should be used for the calculation of forces and power production. However, they only discuss this effect for cases of multiple wind turbines in a grid cell and use high-fidelity simulations to compute a correction factor. A similar approach was suggested by Mayol et al. (2020), who

introduced an induction-aware modification to the Fitch parameterisation by computing a correction factor with idealized WRF  
25 simulations.

The effect of axial induction increases in relevance with increasing ratios between turbine dimensions and grid sizes. It is therefore desirable to have a method that does not rely on precomputed correction factors, but rather one that is directly generalizable. This brief communication proposes a physics-derived modification based on 1D momentum theory. It considers the induction factor of the wind turbine to correct the local grid wind speed back to a free stream wind speed, as is standard  
30 in actuator disc modelling. The validity of the proposed modification is directly verified by comparing the model's power estimations to power curve calculations using the wind speed from a reference simulation without a turbine.

## 2 Methodology

### 2.1 WRF setup

WRF version 4.2.1 was employed for this study. Note that this version already includes the bug fix to the Fitch parameterisation  
35 reported by Archer et al. (2020). The simulation setup was largely based on Cañadillas et al. (2022). Three one-way nested domains, the smallest one having a spatial resolution of 2 km, were centered around a random point in the German Bight. Initial and boundary conditions were described every 6 hours by ERA5, while the sea surface temperature was provided by OSTIA. The physics schemes used consists of the following: the MYNN 2.5 level planetary boundary layer scheme, the Noah Land-Surface model, the MYNN surface layer scheme, the RRTMG long-wave and short-wave radiation schemes, the WRF  
40 Single-Moment 5-class microphysics scheme and the Kain-Fritsch cumulus scheme (only outer two domains).

We conducted a simulation of five days (21-25 January 2020), preceded by 24 hours that were omitted as spin-up. A single turbine was placed in the domain, which was centered around the German Bight. To analyse the sensitivity of the power calculations on the turbine dimensions, two turbine types were used: the NREL 5 MW wind turbine (Jonkman et al., 2009) with a hub height of 90 m and a rotor diameter of 126 m and a 22 MW wind turbine with a hub height of 175 m and a rotor  
45 diameter of 290 m that was created by simple dimensional upscaling of the IEA 15 MW wind turbine (Evan Gaertner et al., 2020). As a reference, a simulation without turbines was performed, from which wind speed time series at hub height were extracted for a direct calculation of power by means of the turbine's power curve.

### 2.2 Fitch modification

The Fitch parameterisation calculates each turbine's power output  $P$  and its influence on the momentum equations using the  
50 following equations:

$$\frac{\partial u}{\partial t} = -0.5 \cdot C_T(u) \cdot u^2 \cdot A \quad (1)$$

$$P = 0.5 \cdot \rho \cdot C_P(u) \cdot u^3 \cdot A \quad (2)$$

$$\frac{\partial \text{TKE}}{\partial t} = -0.5 \cdot C_{\text{TKE}}(u) \cdot u^3 \cdot A \quad (3)$$

with  $u$  the locally sampled wind speed in the grid cell in which the turbine is located,  $C_T$  and  $C_P$  the turbine's wind speed-dependent thrust and power coefficients,  $A = \pi(D/2)^2$  the turbine's rotor area and  $\rho$  a standard air density. The coefficient  $C_{TKE}$ , used to calculate the tendency of the turbulent kinetic energy (TKE), is derived from the known power and thrust coefficients by  $C_{TKE} = C_T - C_P$ . These calculations are done for each turbine individually. When one grid cell contains multiple turbines, the resulting effect on the momentum equations is just a sum of the single turbine contributions.  $C_T$  and  $C_P$  are dependent on a free stream wind speed that is undisturbed by the presence of the turbine. In practice, measurements are taken at least 2.5 rotor diameter upstream of the wind turbine. As the current implementation of the Fitch equations samples the wind speed  $u$  inside the grid cell, this condition is not respected. To this end, we suggest a modification to the Fitch equations that is based on a correction of the local wind speed  $u$  of the grid cell in which the turbine is placed, by the induction factor  $a$  of the wind turbine. The aim is to obtain a free wind speed  $u_\infty$  to be used in power and thrust calculations:

$$u_\infty = \frac{u}{1-a} \quad (4)$$

with

$$a = 0.5(1 - \sqrt{1 - C_T(u_\infty)}) \cdot f(\delta, dx, D) \quad (5)$$

The induction factor  $a$  is calculated from the  $C_T$  of the turbine. A correction function  $f$  is needed to calculate how much of the mesh cross-section is occupied by the turbine area  $A$ . Because turbine orientation and mesh orientation rarely align, we propose the following correction function, which considers the local wind direction  $\delta$  at hub height:

$$f(u, dx, D) = A \cdot (D \cdot dx \cdot \min(|\frac{1}{\cos(\delta)}|, |\frac{1}{\sin(\delta)}|))^{-1} \quad (6)$$

with  $dx$  the horizontal grid size,  $D$  the rotor diameter and  $\delta$  the horizontal wind direction. The correction function  $f$  becomes  $A \cdot (D \cdot dx)^{-1}$  when the wind vector and thus the turbine orientation is perpendicular to the mesh and  $A \cdot (D \cdot \sqrt{2} \cdot dx)^{-1}$  when it is diagonal to the mesh. In the final set of equations, the wind speed variable  $u_\infty$  replaces the locally sampled wind speed  $u$  in the equations 1 to 3.

For  $n$  wind turbines within one grid cell, the wind speed correction can be extended by multiplying each turbine's induction. Note that we consider here that each turbine in the grid cell faces the free wind speed, and no mutual wake interactions occur. The assumption also is only valid when all wind turbines are of the same type.

$$u_\infty = \frac{u}{(1-a)^n} \quad (7)$$

### 3 Results

Figure 1 compares the calculated power of the reference, the original Fitch (Fitch-o), and the induction modification proposed here (Fitch-AIF). Figures 1(a,d) exhibits a reconstructed power curve and (b,e) the difference of both Fitch estimates relative to the reference. The scatter in these plots is due to the divergence between simulations due to e.g., numerical approximations and the chaotic behavior of the atmosphere. Regardless, Fitch-o shows a clear systematic power deviation for wind speeds below

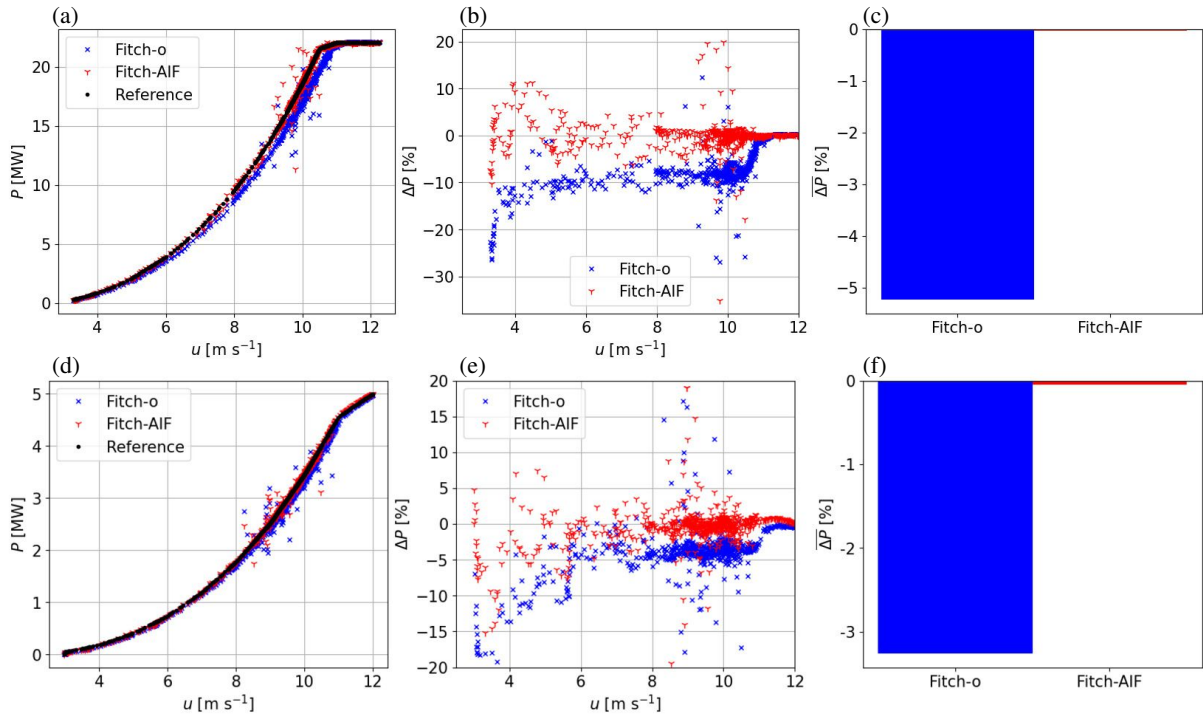


**Figure 1.** Comparison for the 22 MW (a-c) and 5 MW (d-f) turbines modeled with different versions of the Fitch model and the reference. (a,d) Reconstructed power curves. (b,e) Power difference relative to the reference as function of wind speed. (c,f) Mean power difference relative to the reference.

rated, whereas Fitch-AIF exhibits values around zero. Averaged over the 5 day long simulation, Figures 1(c,f) demonstrate that Fitch-o produces a significant error, which vanishes for Fitch-AIF. Besides, the power difference is lower for the smaller turbine, which can be explained by the lower induction effect generated by the smaller turbine. Compared to Fitch-o, Fitch-AIF shows for the wind conditions during the simulated period a mean power and thrust increase of 5.5% and 1.8% respectively for the 22 MW turbine, and 3.3% and 2.0% respectively for the 5 MW turbine. Due to the increased thrust, the wake deficits will also increase.

90 To demonstrate the scalability of the modification with high capacity densities and multiple turbines, five 22 MW wind turbines were placed within a single grid cell in WRF. While this scenario is rather unrealistic, it tests whether the proposed modification holds in extreme cases. Under the assumption that all five turbines operate in free wind conditions, the average power production per turbine calculated with the modification for multiple turbines (Fitch-mAIF) was compared with Fitch-o, Fitch-AIF and the reference (Fig. 2).

95 This exercise reveals that the underestimation of Fitch-o for this extreme dense case of turbines is about 23 %. This reduces to 18 % for Fitch-AIF but is almost eliminated when considering the number of turbines in the grid cell (Fitch-mAIF). The slightly positive  $\overline{\Delta P}$  in Figure 2c is an artifact of the decorrelation of wind speeds between the simulations with and without

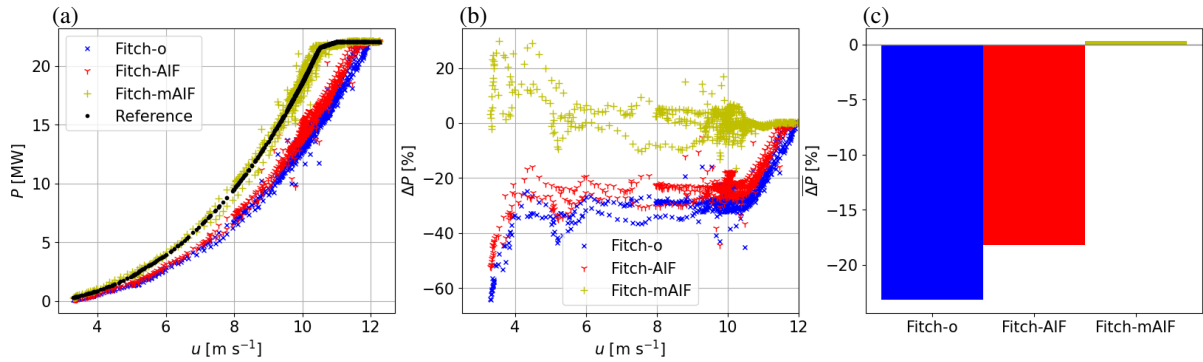


**Figure 2.** Same as in Fig.1 but for five 22 MW turbines per grid cell and with the addition of the Fitch-mAIF modification that combines the induction effect of the turbines within the grid cell for power calculation.

turbines caused by the presence of the turbines. A longer simulation time would effectively eliminate this artifact and therefore does not affect AEP estimates from year-long simulations. Compared to Fitch-o, Fitch-AIF shows a power and thrust increase of 6.4% and 3.3%, while Fitch-mAIF displays increases of 30.6% and 15.1%. By showing that the modification is scalable to even these high capacity and turbine densities, we can infer that it also works for more realistic lower densities.

#### 4 Discussion and conclusions

The Fitch wind farm parameterisation implemented in WRF version 4.2.1 does not consider local induction effects and consequently underestimates power production of a single wind turbine in the dynamic region of the power curve. This issue is amplified for large turbines or when there are multiple turbines in one grid cell. To correct this underestimation, we propose a modification derived from the 1D momentum theory. Instead of using the local wind speed of the grid cell, we use the wind speed dependent induction factor to estimate the free stream wind speed. Results from a simple analysis verify that the turbine's power curve is reproduced when including this modification, thus improving the power estimation of the wind turbine. Compared to measurement data, the power of a turbine will likely still differ from the simulated power by WRF, for example due to biases in the modelled wind speeds and power curves. A full scale validation with measurement data is therefore considered important for future work. With the proposed induction correction, however, the model's negligence about the reduction of wind speed inside the grid cell due to the turbine's presence is not responsible for the difference anymore.

It is important to note that downstream wind speeds from wind farms modelled with WRF-Fitch have shown a good agreement with measurements (Cañadillas et al., 2022; Fischereit et al., 2021). This implies that the Fitch model may be unintentionally generating correct results by ignoring induction as well as wake effects for grid cells containing multiple turbines. Instead of ignoring both effects, the reduction of thrust and power production of the cluster of turbines within a single grid cell due to inner-grid wake effects should be estimated, with the reference wind speed for the calculations being the induction-corrected

wind speed. In this regard, the presented correction is just the first step towards a more correct wind farm parametrisation within mesoscale models.

120 Solving the induction correction becomes challenging when turbines in a grid cell have different dimensions. In such cases, the non-dimensional thrust coefficient needs to be converted to dimensional form and variations in hub heights need to be considered. However, if precise yield calculations for individual turbines are desired, the mesoscale model may not be the most suitable choice due to its low spatial resolution. Regardless, it is worth considering whether increasing the model resolution and allocating more computing resources is worthwhile to mitigate unresolved inner-grid effects.

125 In short, for scenario calculations of wind farm yields with wind farms of not more than one single turbine per cell (e.g., calculations involving future turbine dimensions), we strongly recommend using the proposed modification as presented in this paper for more accurate yield and wind resource assessments.

*Code availability.* The WRF code with the induction correction for the Fitch parameterisation is available for download at <https://github.com/FraunhoferIWES/WRF.git>

130 (<https://doi.org/10.5281/zenodo.12608856>, Sengers et al. (2024)).

*Author contributions.* LV conceptualized the idea, BAMS implemented of the correction in WRF and performed the simulations. MD initiated the associated research project, and was thus involved in the funding acquisition as well as discussions. All authors contributed intensively to the writing and reviewing of the manuscript.

*Competing interests.* The authors declare that there are no competing interests

135 *Acknowledgements.* The results presented in this paper were derived in the framework of the X-Wakes (grant no. 03EE3008) project. The X-Wakes project is funded by the German Federal Ministry for Economic Affairs and Climate Action (Bundesministerium für Wirtschaft und Klimaschutz – BMWK) due to a decision of the German Bundestag. The simulations were partly performed at the HPC Cluster EDDY, located at the University of Oldenburg (Germany) funded by BMWK (grant no. 03240).

## References

- 140 Abkar, M. and Porté-Agel, F.: A new wind-farm parameterization for large-scale atmospheric models, *J. Renew. Sustain. Ener.*, 7, 013–121, <https://doi.org/10.1063/1.4907600>, 2015.
- Archer, C., Wu, S., Ma, Y., and Jimenez, P.: Two Corrections for Turbulent Kinetic Energy Generated by Wind Farms in the WRF Model, *Mon. Wea. Rev.*, 148, 4823–4835, <https://doi.org/10.1175/MWR-D-20-0097.1>, 2020.
- Cañadillas, B., Beckenbauer, M., Trujillo, J. J., Dörenkämper, M., Foreman, R., Neumann, T., and Lampert, A.: Offshore wind farm cluster wakes as observed by long-range-scanning wind lidar measurements and mesoscale modeling, *Wind Energ. Sci.*, 7, 1241–1262, <https://doi.org/10.5194/wes-7-1241-2022>, 2022.
- 145 Evan Gaertner, Jennifer Rinker, Latha Sethuraman, Frederik Zahle, Benjamin Anderson, Garrett Barter, Nikhar Abbas, Fanzhong Meng, Pietro Bortolotti, Witold Skrzypinski, George Scott, Roland Feil, Henrik Bredmose, Katherine Dykes, Matt Shields, Christopher Allen, and Anthony Viselli: Definition of the IEA 15-Megawatt Offshore Reference Wind Turbine, <https://www.nrel.gov/docs/fy20osti/75698.pdf>, 2020.
- 150 Fischereit, J., Brown, R., Larsén, X. G., Badger, J., and Hawkes, G.: Review of Mesoscale Wind-Farm Parametrizations and Their Applications, *Bound.-Lay. Meteorol.*, <https://doi.org/10.1007/s10546-021-00652-y>, 2021.
- Fitch, A. C., Olson, J. B., Lundquist, J. K., Dudhia, J., Gupta, A. K., Michalakes, J., and Barstad, I.: Local and Mesoscale Impacts of Wind Farms as Parameterized in a Mesoscale NWP Model, *Mon. Wea. Rev.*, 140, 3017–3038, <https://doi.org/10.1175/MWR-D-11-00352.1>, 2012.
- 155 Jonkman, J., Butterfield, S., Musial, W., and Scott, G.: Definition of a 5-MW Reference Wind Turbine for Offshore System Development, Tech. Rep. TP-500-38060, National Renewable Energy Laboratory, <https://doi.org/10.2172/947422>, 2009.
- Lundquist, J. K., DuVivier, K. K., Kaffine, D., and Tomaszewski, J. M.: Costs and consequences of wind turbine wake effects arising from uncoordinated wind energy development, *Nature Energy*, 4, 26–34, <https://doi.org/10.1038/s41560-018-0281-2>, 2019.
- 160 Maas, O. and Raasch, S.: Wake properties and power output of very large wind farms for different meteorological conditions and turbine spacings: a large-eddy simulation case study for the German Bight, *Wind Energ. Sci.*, 7, 715–739, <https://doi.org/10.5194/wes-7-715-2022>, 2022.
- Mayol, M., Navarro Diaz, G., Saulo, A., and Otero, A.: An induction-aware parameterization for wind farms in the WRF mesoscale model, *J. Phys.-Conf. Ser.*, 1618, 062 006, <https://doi.org/10.1088/1742-6596/1618/6/062006>, 2020.
- 165 Nygaard, N. G., Steen, S. T., Poulsen, L., and Pedersen, J. G.: Modelling cluster wakes and wind farm blockage, *J. Phys.-Conf. Ser.*, 1618, 062 072, <https://doi.org/10.1088/1742-6596/1618/6/062072>, 2020.
- Sengers, B., Vollmer, L., and Dörenkämper, M.: First release of Axial Induction Factor correction of WRF Fitch in v4.2.1, <https://doi.org/10.5281/zenodo.12608856>, Zenodo [code], 2024.
- Siedersleben, S. K., Platis, A., Lundquist, J. K., Lampert, A., Bärfuss, K., Cañadillas, B., Djath, B., Schulz-Stellenfleth, J., Bange, J., Neumann, T., and Emeis, S.: Evaluation of a Wind Farm Parameterization for Mesoscale Atmospheric Flow Models with Aircraft Measurements, *Meteorol. Z.*, 27, 401–415, <https://doi.org/10.1127/metz/2018/0900>, 2018.
- 170 Skamarock, W. C. and Klemp, J. B.: A time-split nonhydrostatic atmospheric model for weather research and forecasting applications, *Journal of Computational Physics*, 227, 3465–3485, <https://doi.org/10.1016/j.jcp.2007.01.037>, 2008.

- Skamarock, W. C., Klemp, J. B., Dudhia, J., Gill, D. O., Liu, Z., Berner, J., Wang, W., Powers, J. G., Duda, M. G., Barker, D. M., and Huang, X.-Y.: A Description of the Advanced Research WRF Model Version 4.3, Tech. Rep. TN-556+STR, National Center for Atmospheric Research, <https://doi.org/10.5065/1dfh-6p97>, 2021.
- 175 Wiegant, E. and Verzijlbergh, R.: GRASP model description & validation report, [https://www.dutchoffshorewindatlas.nl/binaries/dowa/documenten/reports/2019/12/05/whiffle-report---grasp-model-description-and-validation-report/grasp\\_description\\_validation.pdf](https://www.dutchoffshorewindatlas.nl/binaries/dowa/documenten/reports/2019/12/05/whiffle-report---grasp-model-description-and-validation-report/grasp_description_validation.pdf), last accessed: 19 June 2023, 2019.